American Mineralogist, Volume 80, pages 329–335, 1995

# Site preference of rare earth elements in fluorapatite

MICHAEL E. FLEET
Department of Earth Sciences, University of Western Ontario, London, Ontario N6A 5B7, Canada
YUANMING PAN
Department of Geological Sciences, University of Saskatchewan, Saskatoon, Saskatchewan S7N 0W0, Canada

## ABSTRACT

Crystals of La-, Gd-, and Dy-bearing fluorapatite [La-FAp, Gd-FAp, Dy-FAp; $Ca_{10-x-2y}Na_yREE_{x+y}(P_{1-x}Si_xO_4)_6A_2$, with $x = 0.24$–$0.29$, $y = 0.32$–$0.36$; $P6_3/m$] have been synthesized hydrothermally, and their structures refined at room temperature with single-crystal X-ray intensities to $R = 0.015$–$0.018$. Na is essentially restricted to the Ca1 position in La-FAp, Gd-FAp, and Dy-FAp, in contrast to Nd-FAp, which was synthesized under slightly different conditions and has appreciable Na in Ca2 as well. Site occupancies for REE in Ca1 and Ca2, respectively, are 0.023(1) and 0.093(1) in LaFAp, 0.038(1) and 0.111(1) in Nd-FAp, 0.038(0) and 0.077(0) in Gd-FAp, and 0.039(1) and 0.060(1) in Dy-FAp. The REE site occupancy ratio (REE-Ca2 to REE-Ca1) appears to decrease monotonically for $REE^{3+}$ cations through the 4f transition-metal series. With this assumption, site occupancy ratios (REE-Ca2 to REE-Ca1) for some other REE in natural apatite are estimated to be: La 4.04, Ce 3.67, Pr 3.30, Nd 2.92, Sm 2.47, Eu 2.25, Gd 2.03, Dy 1.54, Y 1.29, Er 1.05. These single-REE site occupancy ratios may not be transferrable to natural apatite.

The Ca1 and Ca2 site occupancies are generally consistent with site preferences deduced from bond-valence calculations, which show that the substitutions for Ca lead to equalization of Ca1 and Ca2 bond valences. Also, the REE site occupancy ratio correlates inversely with F bond valence.

## INTRODUCTION

The crystal chemical behavior of rare earth elements (REE) in minerals is largely controlled by the substitution of these elements at Ca structural positions, modified by the monotonic decrease in their ionic radii with the increase in atomic number (La → Lu; e.g., McKay, 1989; Burt, 1989; Miyawaki and Nakai, 1993). The atomic radii of REE diminish steadily toward the heavy end of the 4f transition-metal series because of the progressive increase in nuclear charge. Thus, the selectivity of Ca-bearing minerals for REE is greatly dependent on the size of the Ca positions in individual mineral structures. Light REE (LREE) are typically concentrated in minerals with large Ca positions (e.g., allanite), middle REE (MREE) in minerals with medium-sized Ca positions (e.g., clinopyroxene), and heavy REE (HREE) in minerals with small Ca positions (e.g., garnet). Bonding effects may exert considerable influence as well. However, the splitting of the energies of the 4f orbitals in electrostatic ligand fields is very small ($\Delta_o$ for octahedral fields is usually about 1 kJ/mol); thus crystal field stabilization energies (CFSE) are relatively unimportant in REE crystal chemistry (e.g., Morss, 1976).

Apatite [$Ca_{10}(PO_4)_6A_2$, A = F, OH, Cl; space group $P6_3/m$, but $P2_1/b$ for some ordered varieties] is an important host mineral for REE in igneous, metamorphic, and sedimentary rocks, and REE-doped apatites have important technological applications (e.g., lasers and luminescent materials: Mackie and Young, 1973; Gunawardane et al., 1982). The two Ca positions in the atomic arrangement of apatite have distinct stereochemistries (Ca1, equipoint 4*f*, $CaO_9$ tricapped trigonal prism; Ca2, equipoint 6*h*, $CaO_6A$ irregular polyhedron; Fig. 1; see Fig. 1 of Hughes et al., 1991, and Fig. 1 of Fleet and Pan, 1994, for further details of stereochemical environments of Ca1 and Ca2), and are able to accommodate a variety of univalent, divalent, and trivalent cations as substituents (e.g., Kay et al., 1964; Mackie et al., 1972; Elliott et al., 1973; Hughes et al., 1989, 1990, 1991; Hughson and Sen Gupta, 1964; Cockbain and Smith, 1967; Mackie and Young, 1973; Gunawardane et al., 1982; Suitch et al., 1985; Rønsbo, 1989; Wyckoff, 1965). As recently summarized in Fleet and Pan (1994), substitution of trivalent REE in apatite is principally compensated as follows:

$$REE^{3+} + Si^{4+} = Ca^{2+} + P^{5+};$$
$$Ca_{10-x}REE_x(P_{1-x}Si_xO_4)_6A_2 \quad (1)$$

$$REE^{3+} + Na^{1+} = 2Ca^{2+};$$
$$Ca_{10-2y}Na_yREE_y(PO_4)_6A_2 \quad (2)$$

0003–004X/95/0304–0329$02.00

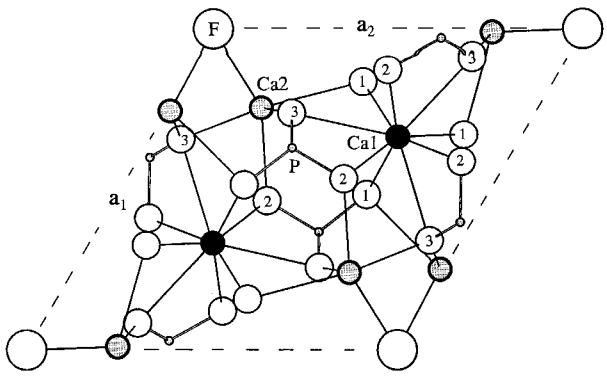


Fig. 1. Structure of fluorapatite showing interrelations of Ca1 and Ca2 polyhedra: O atoms are medium-sized open circles; equivalent Ca2-O3 bonds overlap in c-axis projection.

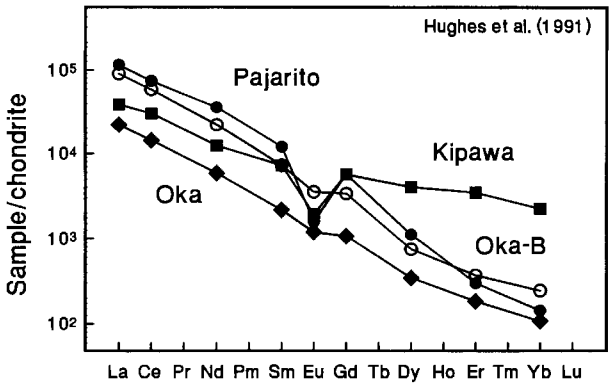


Fig. 2. Chondrite-normalized plot illustrating REE compositions of four natural apatites studied by Hughes et al. (1991).

$$REE^{3+} + O^{2-} = Ca^{2+} + A^{1-}; \qquad Ca_{10-z}REE_z(PO_4)_6A_{2-z}O_z \quad (3)$$

$$2REE^{3+} + \square = 3Ca^{2+}; \qquad Ca_{10-3w}REE_{2w}\square_w(PO_4)_6A_2. \quad (4)$$

The partitioning of the REE between the two Ca positions in apatite contradicts the usual first-order dependence on spatial accommodation, with LREE in particular favoring the smaller Ca2 position. This behavior has been variously ascribed to a control by substitution mechanism (Mackie and Young, 1973), electronegativity difference (Urusov and Khudolozhkin, 1974), and bond valence (Hughes et al., 1991; Fleet and Pan, 1994).

The preference of individual REE among multiple Ca positions in minerals (site occupancy of individual REE) has not been extensively studied because of the inability of conventional diffraction methods to distinguish among individual elements on multiply occupied sites. We have reproduced the REE contents of the four natural apatites studied by Hughes et al. (1991) in Figure 2 to emphasize the extent of this problem for natural samples. These LREE-enriched patterns are typical of apatite from alkaline igneous rocks and pegmatites. Hughes et al. (1991) estimated site preferences for individual LREE from theoretical bond-valence sums, reasoning that La → Pr should preferentially substitute into Ca2, whereas Pm → Sm should selectively substitute into Ca1.

We report X-ray structure site occupancies for three synthetic fluorapatites with single REE substitutions (La-FAp, Gd-FAp, and Dy-FAp). Recent refinement of the structure of a Nd-substituted fluorapatite (Nd-FAp) showed that 80 at% of the Nd was partitioned into Ca2, in general agreement with the Hughes et al. (1991) analysis (Fleet and Pan, 1994). We have marginally improved this refinement and include it in the present study for continuity.

## Experimental procedures

Single crystals of REE-substituted fluorapatite were grown from a volatile-rich melt using a standard cold-seal hydrothermal reaction vessel. The starting material was a stoichiometric mixture of tribasic calcium phosphate [~$Ca_{10}(PO_4)_6(OH)_2$; synthetic hydroxylapatite], $REE_2O_3$ (99.99 wt%), and high-purity $CaF_2$ and amorphous $SiO_2$ (all supplied by Aldrich Chemical Company), containing the equivalent of about 10 mol% $Ca_4REE_6(SiO_4)_6F_2$. Charges consisted of about 0.040 g of the starting composition, 0.040 g of NaF and 0.01 $cm^3$ of deionized $H_2O$ contained in a sealed Au capsule about 4 cm in length. Nd-FAp (Fleet and Pan, 1994) was heated to 940 °C at 0.17 GPa for 2 h and cooled stepwise to the experiment temperature (Table 1). La-FAp, Gd-FAp, and Dy-FAp were heated to 900 °C at 0.17 GPa and cooled at 0.1 °/min to the experiment temperature (Table 1). All charges were quenched in air and $H_2O$. Crystal growth was initiated on the cooling gradient, and the extent of annealing and recrystallization at the experiment temperature is unknown. However, none of the single-crystal products exhibited a core to margin gradation in composition.

The synthetic apatite crystals were analyzed using JEOL JXA-8600 Superprobes at the Universities of Western Ontario and Saskatchewan. Operating conditions included an accelerating voltage of 25 kV, a beam current of 20 nA, a beam diameter of 2–5 μm, 20-s counts, and minerals and synthetic glasses as standards (cf. Pan and Fleet, 1990). The compositions reported in Table 2 are averages of at least 10–12 individual spot analyses. A weak oscillatory compositional growth zoning was evident in electron backscattered images, but the standard deviations of the quantitative analyses (Table 2) were within acceptable limits for X-ray structure refinement.

Single-crystal measurements were made with an Enraf Nonius CAD-4F diffractometer, using graphite monochromatized Mo$K\alpha$ X-radiation. Structure refinements followed Fleet and Pan (1994), and experimental details are given in Table 1. The idealized formulae assumed for refinement are given in Table 2; scattering factors for neutral atomic species and values of f′ and f″ were taken, respectively, from Tables 2.2B and 2.3.1 of the *International Tables for X-ray Crystallography* (Ibers and Ham-

**TABLE 1.** Experimental details

| | La-FAp | Nd-FAp | Gd-FAp | Dy-FAp |
|---|---|---|---|---|
| | **Synthesis** | | | |
| Expt. | AP16 | AP5 | AP13 | AP41 |
| $T$ (°C) | 700 | 685 | 700 | 685 |
| $P$ (GPa) | 0.11 | 0.11 | 0.12 | 0.11 |
| $t$ (h) | 48 | 36 | 42 | 16 |
| | **Crystal data** | | | |
| Size (mm³ × 10³) | 0.73 | 0.96 | 1.68 | 1.08 |
| $a$ (Å) | 9.4123(9) | 9.3979(13) | 9.3853(10) | 9.3784(7) |
| $c$ (Å) | 6.9080(14) | 6.8997(8) | 6.8876(11) | 6.8832(6) |
| $V$ (Å³) | 530.01 | 527.71 | 525.36 | 524.26 |
| No. of refl. | 20 | 20 | 20 | 20 |
| $2\theta$ range (°) | 51.4–76.1 | 51.4–76.2 | 51.5–76.3 | 51.5–76.4 |
| | **Intensity data** | | | |
| Method | $\theta$-$2\theta$ | $\theta$-$2\theta$ | $\theta$-$2\theta$ | $\theta$-$2\theta$ |
| Refl. | $\pm hkl$ | $\pm hkl$ | $\pm hkl$ | $\pm hkl$ |
| No. of refl. | 3618 | 3594 | 3572 | 3570 |
| No. of unique refl. | 1091 | 1081 | 1077 | 1075 |
| No. with $I < 3\sigma_I$ | 329 | 325 | 245 | 275 |
| Refined parameters | 41 | 41 | 41 | 41 |
| $2\theta$ range (°) | 0–80 | 0–80 | 0–80 | 0–80 |
| | **Absorption correction** | | | |
| $\mu$ (cm⁻¹) | 40.0 | 45.7 | 47.0 | 46.1 |
| Trans. factors* | 0.73–0.76 | 0.32–0.78 | 0.61–0.67 | 0.62–0.68 |
| | **Final refinement** | | | |
| $R$ | 0.018 | 0.024 | 0.015 | 0.017 |
| $R_w$ | 0.017 | 0.025 | 0.015 | 0.017 |
| s | 0.604 | 0.847 | 0.595 | 0.650 |
| Extinction (g** × 10⁴) | 0.606(8) | 1.11(2) | 0.56(1) | 0.611(7) |
| $\Delta\rho$ ($e$/Å³) (+) | 1.16 | 1.02 | 0.54 | 0.46 |
| (−) | 0.54 | 0.84 | 0.36 | 0.46 |

* Determined by Gaussian integration with a 12 × 12 × 12 grid.
** Type I extinction (Coppens and Hamilton, 1970).

**TABLE 2.** Compositions of synthetic REE-bearing fluorapatite

| Apatite | La-FAp | Nd-FAp | Gd-FAp | Dy-FAp |
|---|---|---|---|---|
| $P_2O_5$ (wt%) | 37.68(32) | 34.47(41) | 37.63(58) | 38.29(51) |
| $SiO_2$ | 1.63(7) | 1.80(13) | 1.58(13) | 1.35(31) |
| $REE_2O_3$ | 9.93(74) | 12.74(54) | 10.36(54) | 9.08(35) |
| CaO | 47.54(22) | 44.68(37) | 47.55(44) | 48.20(21) |
| $Na_2O$ | 1.04(2) | 1.47(16) | 1.01(10) | 0.92(15) |
| F | 3.00(9) | 2.87(18) | 2.89(11) | 3.25(7) |
| O ≡ F | 1.26 | 1.21 | 1.22 | 1.37 |
| Total | 99.56 | 99.81 | 99.80 | 99.71 |
| | **Chemical formulae based upon 16 cations** | | | |
| P | 5.656 | 5.710 | 5.672 | 5.750 |
| Si | 0.288 | 0.324 | 0.282 | 0.240 |
| Ca | 9.046 | 8.632 | 9.086 | 9.176 |
| REE | 0.650 | 0.820 | 0.612 | 0.518 |
| Na | 0.358 | 0.512 | 0.348 | 0.316 |
| F | 1.682 | 1.634 | 1.628 | 1.832 |
| OH* | 0.318 | 0.366 | 0.372 | 0.168 |
| O | 23.92 | 24.04 | 23.92 | 23.97 |
| | **Formulae used in X-ray structure refinement** | | | |
| Ca | 9.00 | 8.66 | 9.04 | 9.18 |
| Na | 0.36 | 0.51 | 0.35 | 0.32 |
| REE | 0.65 | 0.82 | 0.61 | 0.52 |
| P | 5.71 | 5.68 | 5.72 | 5.75 |
| Si | 0.29 | 0.32 | 0.28 | 0.24 |
| O | 24.00 | 24.00 | 24.00 | 24.00 |
| F | 2.00 | 2.00 | 2.00 | 2.00 |

* OH calculated by difference.

ilton, 1974). Further details are discussed below. Final parameters are given in Tables 3 and 4, and observed and calculated structure factors in Table 5.[1]

## DISCUSSION

### Determination of site occupancies

The present synthetic apatites were fluorapatite with a single REE substitution, with 1.63–1.83 F anions pfu (Table 2). The structure refinements assumed ideal F end-member compositions.

The REE contents varied from 0.52 to 0.82 cations pfu, somewhat less than the proportion in the bulk starting composition, with a maximum at Nd-FAp. These single-REE contents are comparable with the total REE contents of two of the natural apatites investigated by Hughes et al. (1991), Kipawa and Oka-B, with 0.61 and 0.85 cations pfu, respectively. The substitution of REE in the present synthetic apatites is accommodated exclusively by compensating substitutions of Si and Na (substitution mechanisms 1 and 2; cf. Rønsbo, 1989), with the latter being slightly more dominant. The Na-Si cation ratio varied from 1.23 for Gd-FAp to 1.58 for Nd-FAp. In contrast, the natural apatites studied by Hughes et al. (1991) varied markedly in Na-Si ratio; from Pajarito at 2.97, to Kipawa at 0.23, to Oka-B at 0.05, to Oka at 0.05.

For the structure refinement, Si was assigned a partial occupancy on the P position. However, the structural role of Na presented a problem because the occupancies of REE and Na on the Ca1 and Ca2 positions cannot be varied independently during least-squares refinement with structure factors from Mo$K\alpha$ X-ray intensities alone. The Ca1 position seems to be generally favored by Na, but this preference might be composition dependent and cannot be assumed for apatites of complex composition grown at high temperature. Hughes et al. (1991) addressed this problem by assigning all Na to the Ca1 position, to provide a limiting case for REE ordering. We now follow the procedure of Fleet and Pan (1994), who determined a value for the Na occupancy of Nd-FAp by iteration, with the Na occupancy reset between refinements. However, Fleet and Pan (1994) minimized the conventional residual index ($R$). Minimization of the weighted residual index ($R_w$) at constant Na occupancy is more rigorous and has been adopted in the present study. The new refinement of Nd-FAp is unchanged within the estimated errors but has been included in the present study for continuity and completeness.

Refined occupancies for REE and derived occupancies for Na for the four apatites studied are reported in column 2 of Table 6. Only Nd-FAp has an appreciable content of Na in the Ca2 position. Na is restricted to Ca1 in

[1] A copy of Tables 4 and 5 may be ordered as Document AM-95-584 from the Business Office, Mineralogical Society of America, 1130 Seventeenth Street NW, Suite 330, Washington, DC 20036, U.S.A. Please remit $5.00 in advance for the microfiche.

**TABLE 3.** Atomic positional and isotropic displacement parameters (Å²)

| | | La-FAp | Nd-FAp | Gd-FAp | Dy-FAp |
|---|---|---|---|---|---|
| Ca1 | *x* | ⅔ | ⅔ | ⅔ | ⅔ |
| | *y* | ⅓ | ⅓ | ⅓ | ⅓ |
| | *z* | 0.0006(1) | 0.0000(1) | 0.00033(7) | 0.00049(9) |
| | $B_{eq}$ | 0.88(2) | 0.89(3) | 0.80(1) | 0.79(2) |
| Ca2 | *x* | 0.98989(6) | 0.99024(9) | 0.99174(4) | 0.99242(5) |
| | *y* | 0.24018(6) | 0.24085(9) | 0.24226(4) | 0.24285(5) |
| | *z* | ¼ | ¼ | ¼ | ¼ |
| | $B_{eq}$ | 0.804(8) | 0.75(1) | 0.643(6) | 0.614(7) |
| P | *x* | 0.36898(7) | 0.3687(1) | 0.36842(5) | 0.36839(6) |
| | *y* | 0.39808(7) | 0.3975(1) | 0.39729(5) | 0.39744(6) |
| | *z* | ¼ | ¼ | ¼ | ¼ |
| | $B_{eq}$ | 0.538(8) | 0.52(1) | 0.465(6) | 0.434(7) |
| O1 | *x* | 0.4847(2) | 0.4830(3) | 0.4836(1) | 0.4838(2) |
| | *y* | 0.3268(2) | 0.3253(3) | 0.3251(2) | 0.3252(2) |
| | *z* | ¼ | ¼ | ¼ | ¼ |
| | $B_{eq}$ | 1.01(2) | 0.96(3) | 0.93(2) | 0.88(2) |
| O2 | *x* | 0.4663(2) | 0.4661(3) | 0.4670(1) | 0.4669(2) |
| | *y* | 0.5872(2) | 0.5859(3) | 0.5873(1) | 0.5874(2) |
| | *z* | ¼ | ¼ | ¼ | ¼ |
| | $B_{eq}$ | 1.19(3) | 1.23(4) | 1.08(2) | 1.01(2) |
| O3 | *x* | 0.2568(1) | 0.2561(2) | 0.2560(1) | 0.2561(1) |
| | *y* | 0.3406(2) | 0.3406(2) | 0.3406(1) | 0.3408(1) |
| | *z* | 0.0716(2) | 0.0714(2) | 0.0707(1) | 0.0711(1) |
| | $B_{eq}$ | 1.40(2) | 1.40(3) | 1.30(1) | 1.15(2) |
| F | *x* | 0 | 0 | 0 | 0 |
| | *y* | 0 | 0 | 0 | 0 |
| | *z* | ¼ | ¼ | ¼ | ¼ |
| | $B_{eq}$ | 3.05(8) | 2.94(12) | 2.46(6) | 2.28(7) |

*Note:* $B_{eq} = \frac{1}{3} \Sigma_i \Sigma_j \beta_{ij} \mathbf{a}_i \mathbf{a}_j$.

**TABLE 6.** Refined REE site occupancies

| Position | Cation | 1 | 2 | 3 |
|---|---|---|---|---|
| | | **La-FAp** | | |
| Ca1 | Ca | 0.888 | 0.888 | 0.993 |
| | Na | 0.089 | 0.089 | 0.0 |
| | La | 0.023(1) | 0.023(1) | 0.007(1) |
| Ca2 | Ca | 0.907 | 0.907 | 0.837 |
| | Na | 0.0 | 0.0 | 0.059 |
| | La | 0.093(1) | 0.093(1) | 0.103(1) |
| La in Ca2 (%) | | 86 | 86 | 96 |
| *R* index | | 0.01840 | 0.01840 | 0.01842 |
| | | **Nd-FAp** | | |
| Ca1 | Ca | 0.823 | 0.901 | 0.971 |
| | Na | 0.128 | 0.061 | 0.0 |
| | Nd | 0.049(1) | 0.038(1) | 0.029(1) |
| Ca2 | Ca | 0.896 | 0.843 | 0.797 |
| | Na | 0.0 | 0.045 | 0.086 |
| | Nd | 0.104(1) | 0.111(1) | 0.118(1) |
| Nd in Ca2 (%) | | 76 | 81 | 86 |
| *R* index | | 0.02365 | 0.02362 | 0.02370 |
| | | **Gd-FAp** | | |
| Ca1 | Ca | 0.874 | 0.886 | 0.973 |
| | Na | 0.087 | 0.076 | 0.0 |
| | Gd | 0.039(0) | 0.038(0) | 0.027(0) |
| Ca2 | Ca | 0.924 | 0.916 | 0.858 |
| | Na | 0.0 | 0.007 | 0.058 |
| | Gd | 0.076(0) | 0.077(0) | 0.084(0) |
| Gd in Ca2 (%) | | 75 | 75 | 82 |
| *R* index | | 0.01473 | 0.01472 | 0.01477 |
| | | **Dy-FAp** | | |
| Ca1 | Ca | 0.882 | 0.882 | 0.971 |
| | Na | 0.079 | 0.079 | 0.0 |
| | Dy | 0.039(1) | 0.039(1) | 0.029(1) |
| Ca2 | Ca | 0.940 | 0.940 | 0.880 |
| | Na | 0.0 | 0.0 | 0.053 |
| | Dy | 0.060(1) | 0.060(1) | 0.067(1) |
| Dy in Ca2 (%) | | 70 | 70 | 78 |
| *R* index | | 0.01726 | 0.01726 | 0.01762 |

*Note:* 1 = all Na in Ca1; 2 = Na occupancy defined by iterative refinement; 3 = all Na in Ca2.

La-FAp and Dy-FAp and essentially restricted to Ca1 in Gd-Ap, consistent with the Na site preference deduced from consideration of bond valence (Fleet and Pan, 1994). These three apatites were synthesized under closely comparable conditions that had been established by previous experimentation. The Nd-FAp, however, was from an earlier experiment (AP5), in which the starting composition and NaF were not premixed, the preheating temperature was higher, and the cooling gradient was approximated by manually stepping down the controlling temperature. A later synthesis of Nd-FAp (AP15), following the procedure for La-FAp, Gd-FAp, and Dy-FAp, resulted in a slightly reduced uptake of Nd and a marked reduction in the Na-Si cation ratio (0.97; cf. 1.58 for AP5). Thus, the higher Na occupancy in Ca2 for the present Nd-FAp may be related to the higher Na-Si ratio or different experimental procedures.

Occupancies for refinement of the two limiting models, with all Na on Ca1 and Ca2, respectively, are given in Table 6 for comparison. We have not attempted to evaluate the *R* values for the refinements of Table 6, and indeed they are statistically similar using the Hamilton (1965) test. However, as Fleet and Pan (1994) noted, the Hamilton test may not be applicable to this problem because the variable parameters and observations remain unchanged in the refinements being compared.

In each of the present synthetic apatites, the REE is strongly but not exclusively partitioned into Ca2. Moreover, REE occupancy varies systematically with REE composition; proportional occupancy of Ca2 and the ratio of REE-Ca2 to REE-Ca1 decrease progressively from 86% and 4.04 in La-FAp, to 81% and 2.92 in Nd-FAp, to 75 and 2.03 in Gd-FAp, to 70% and 1.54 in Dy-FAp. Thus, there appears to be a progressive change in REE site preference through the 4f transition-metal series. Assuming this to be the case, single-REE site occupancy ratios (REE-Ca2 to REE-Ca1) for the more abundant REE in apatite (see Fig. 2) are estimated by a combination of measurement and linear interpolation to be La 4.04, Ce 3.67, Pr 3.30, Nd 2.92, Sm 2.47, Eu 2.25, Gd 2.03, Dy 1.54, Y 1.29, Er 1.05, where Y is positioned on the basis of the similarity of $R^{3+}$ with Ho. However, comparison with the refined occupancies of Hughes et al. (1991) suggests that these single-REE site occupancy ratios may not be quantitatively transferrable to natural apatites. REE site occupancy ratios have been calculated for the four natural apatites of Hughes et al. (1991) using the mineral formulae in their Appendix 1, and are compared, respectively, with the observed ratios as follows: Pajarito 3.55 (calc) and 1.76 (obs), Oka-B 3.64 (calc) and 2.10 (obs), Kipawa 3.17 (calc) and 1.97 (obs), Oka 3.54 (calc) and 3.00 (obs). Clearly, only the Oka sample, with the lowest REE abundance (0.33 cations pfu), yields comparable

TABLE 7. Selected bond distances (Å) and angles (°)

| | La-FAp | Nd-FAp | Gd-FAp | Dy-FAp |
|---|---|---|---|---|
| Ca1-O1 × 3 | 2.408(1) | 2.415(1) | 2.405(1) | 2.401(1) |
| Ca1-O2[a] × 3 | 2.462(1) | 2.460(2) | 2.457(1) | 2.455(1) |
| Ca1-O3[a] × 3 | 2.824(1) | 2.817(2) | 2.813(1) | 2.810(1) |
| Mean | 2.565 | 2.564 | 2.558 | 2.555 |
| Ca2-O1[b] | 2.679(1) | 2.662(2) | 2.669(1) | 2.672(1) |
| Ca2-O2[c] | 2.397(1) | 2.391(1) | 2.368(0) | 2.363(0) |
| Ca2-O3 × 2 | 2.520(1) | 2.510(1) | 2.498(1) | 2.491(1) |
| Ca2-O3[d] × 2 | 2.356(1) | 2.352(2) | 2.345(1) | 2.348(1) |
| Mean | 2.471 | 2.463 | 2.454 | 2.452 |
| Ca2-F | 2.310(1) | 2.311(1) | 2.313(0) | 2.314(0) |
| P-O1 | 1.538(2) | 1.531(2) | 1.536(1) | 1.537(1) |
| P-O2 | 1.542(2) | 1.534(3) | 1.545(1) | 1.543(1) |
| P-O3 × 2 | 1.535(1) | 1.535(1) | 1.537(1) | 1.532(1) |
| Mean | 1.538 | 1.534 | 1.539 | 1.536 |
| O1-P-O2 | 111.21(10) | 111.46(15) | 111.20(7) | 111.21(9) |
| O1-P-O3[e] × 2 | 111.03(6) | 111.06(9) | 111.11(4) | 111.11(5) |
| O2-P-O3 × 2 | 108.28(6) | 108.16(10) | 108.13(4) | 108.14(5) |
| O3-P-O3[e] | 106.85(9) | 106.75(14) | 107.00(7) | 106.96(8) |

*Note:* a = $-x, -y, -z$; b = $-y, x-y, z$; c = $y-x, -x, z$; d = $x-y, x, -z$; e = $x, y, \frac{1}{2}-z$.

TABLE 8. Bond valences*

| | La-FAp | Nd-FAp | Gd-FAp | Dy-FAp | FAp** |
|---|---|---|---|---|---|
| Ca1 | 1.947 | 1.930 | 1.947 | 1.955 | 2.016 |
| Ca2 | 1.979 | 1.962 | 1.960 | 1.946 | 1.878 |
| P | 5.037 | 5.090 | 5.020 | 5.059 | 5.065 |
| O1 | 1.990 | 2.005 | 1.991 | 1.989 | 1.995 |
| O2 | 2.061 | 2.084 | 2.057 | 2.066 | 2.072 |
| O3 | 1.974 | 1.969 | 1.963 | 1.976 | 1.960 |
| F | 0.950 | 0.932 | 0.911 | 0.902 | 0.895 |

* After Brown (1981).
** Bond distances from Hughes et al. (1989).

values for calculated and observed ratios. Because the absolute REE abundances of the natural apatites peak at La-Ce-Nd, calculated values are expected to be in the range of 3.0–3.5, and the Kipawa sample, with the flattest REE pattern (Fig. 2), has the lowest calculated value. These discrepancies between calculated and observed REE occupancy ratios are apparently not attributable to other compositional variables. Although the present synthetic apatites have rather restricted compositions, the compositions of the four natural apatites of Hughes et al. (1991) span broad ranges in Na-Si cation and F-OH anion ratios.

### Variation in bond distances

In natural apatite, substitution of LREE in preference to HREE (cf. Fig. 2) results in an increase in the size of the structure (Hughes et al., 1991). This is because, for a given stereochemical environment, $R^{3+}$ of La and Ce is greater than $R^{2+}$ of Ca, the latter generally corresponding to $R^{3+}$ of Nd. For the present synthetic apatites, unit-cell volume and bond distances generally decrease from La-FAp to Dy-FAp, as expected. However, the structural parameters for end-member fluorapatite (Hughes et al., 1989; cell volume 526.03 Å$^3$) are in closer agreement with Gd-FAp than Nd-FAp.

The effect of substitution of REE and Na into fluorapatite may be evaluated by calculating the ideal Ca1-O and Ca2-O bond distances using the site occupancies in column 2 of Table 6 and the ionic radii for eightfold coordination (Shannon, 1976): for La-FAp to Dy-FAp, these are 2.527, 2.523, 2.522, and 2.521 Å, respectively, for Ca1, and 2.524, 2.520, 2.515, and 2.515 Å, respectively, for Ca2. Mean Ca-O bond distances for Ca1 and Ca2 positions (Table 7) do correlate approximately linearly with these calculated ideal distances, but with slopes of about 2:1 for both Ca1 and Ca2. These correlations are independent of the specific coordination assumed in the calculation of ideal Ca1-O and Ca2-O distances. Thus, the progressive decrease in Ca-O distance through the series of La-FAp to Dy-FAp is greater by a factor of about two than that predicted from ideal bond distances. This is partly compensated by a progressive increase in the Ca2-F bond distance (Fig. 3, Table 7), which we attribute below to a progressive decrease in bond valence. Further inspection of the data in Table 7 reveals that some Ca-O bond distances vary erratically with REE substitution. The Ca-O distances that more closely reflect overall structural change with REE substitution are plotted in Figure 3.

### Controls on REE site occupancy

The major controls on REE site occupancy remain unclear. Bonding requirement as estimated by bond valence is certainly an important factor. More generally, calculated bond valence is indeed a very powerful first-approximation technique for deducing REE site preference of end-member calc-silicate structures (Fleet and Pan, in preparation). However, bond-valence calculations are based on the correlation between bond distance and bond strength and therefore also embody a component attributed to variation in size of structural positions. This coupling of the effects of bond valence and substituent size gives rise to an ambiguity in interpretation that is particularly troublesome where bond valence is calculated for multiply occupied sites, as in the present synthetic apatites (Table 8), for which the experimental bond distance is biased toward that of the substituent with the stronger X-ray scattering contribution.

Fleet and Pan (1994) pointed out that the Ca2 position in end-member fluorapatite is underbonded (Table 8). Therefore, minor amounts of trivalent REE should favor Ca2 over Ca1, to increase the bond valences of both Ca2 and F. Conversely, Na should then favor Ca1. We suggested that the bond valence requirements of the A (or O) anion alone must exert a considerable influence on the site preference of cations in apatites, in concert with the strong preference of trivalent REE for the Ca2 position in oxyapatites (Gunawardane et al., 1982) and $Nd_2O_3$-doped fluorapatite (Mackie and Young, 1973).

Hughes et al. (1991) used calculated bond valence to show that heavy REE (Gd → Lu) are underbonded in either Ca position, whereas La, Ce, and Pr are slightly overbonded in the Ca1 position and therefore should prefer Ca2, Pm and Sm should favor Ca1, and Nd should

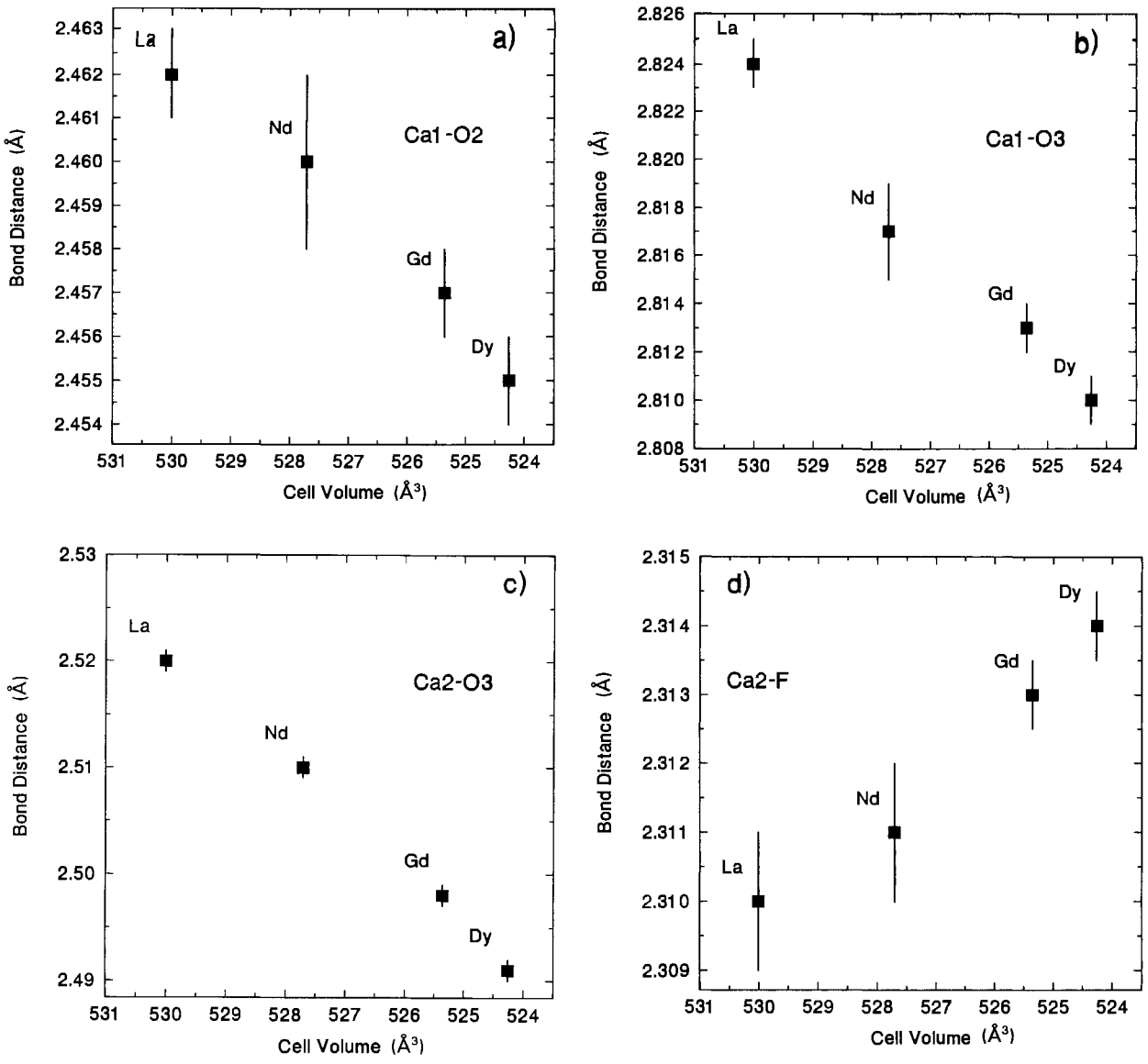


Fig. 3. (**a**–**d**) Ca-O distances reflecting overall structural change with REE substitution in four synthetic fluorapatite samples, La-FAp, Nd-FAp, Gd-FAp, and Dy-FAp.

readily substitute into either Ca1 or Ca2. Conversely, the present X-ray refinements reveal an apparent monotonic decrease in REE site occupancy ratio (REE-Ca2 to REE-Ca1) through the 4f transition-metal series. The bond valences of Ca1 and Ca2 do remain more or less equal, but that of F progressively decreases to a value for Dy-FAp that is very similar to the value for fluorapatite (Table 8). Because the Ca2-F distance is only weakly constrained by the apatite structure, the F bond valence does reflect the REE site occupancy ratio and is inversely correlated with it, as is illustrated in Figure 4.

In summary, there remain problems in understanding the crystal-chemical controls on REE site occupancy in apatites. The monotonic decrease in the ratio of REE-Ca2 to REE-Ca1 through the 4f transition-metal series could be attributed to equalization of Ca1 and Ca2 bond valences. However, as with most other aspects of REE crystal chemistry, the controlling factor could be spatial accommodation of trivalent REE in Ca positions, with site preference changing progressively in response to the monotonic decrease in $R^{3+}$, and the smaller HREE cations more readily accommodated in Ca1. Fleet and Pan (1994) noted that a simple average of bond lengths gives a misleading estimate of the relative sizes of the Ca polyhedra in the apatite structure because the coordination of Ca1 is really 6+3 rather than 9. The six closest O atoms to Ca1 (O1, O2; Fig. 1) form a trigonal prismatic cluster, sharing basal faces to link into chains parallel to the c

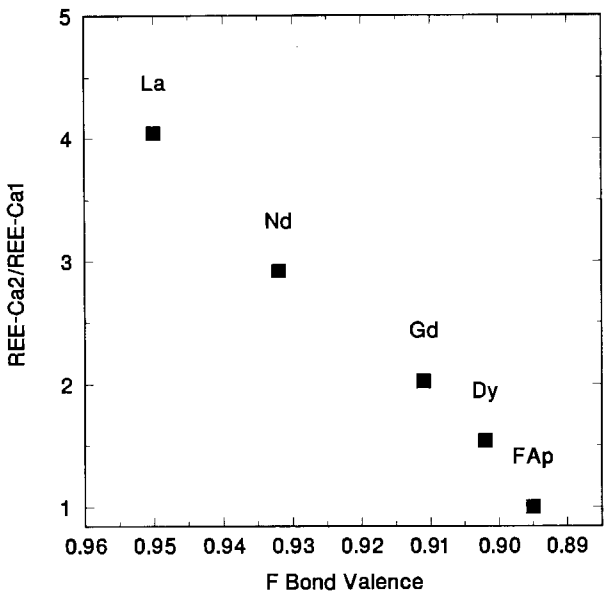


Fig. 4. Inverse correlation between REE site occupancy ratio (REE-Ca2 to REE-Ca1) and F bond valence in La-FAp, Nd-FAp, Gd-FAp, Dy-FAp, and FAp: FAp is fluorapatite from Hughes et al. (1989).

axis. Hence, the effective size of Ca1 with respect to spatial accommodation of REE may be less than that of Ca2. This discussion emphasizes the difficulty of estimating the effective size of large cation positions in structures, and indeed the effective radius of the bonding sphere of these cations is often defined somewhat arbitrarily as well. For similar starting compositions, the uptake of REE by fluorapatite falls off abruptly beyond Dy-FAp (Fleet and Pan, in preparation). Thus, the decrease in the ratio of REE-Ca2 to REE-Ca1 may reflect progressive incompatibility between trivalent HREE and the stereochemical environment of Ca2, rather than an increasing preference for Ca1.

## Acknowledgments

We thank J.M. Hughes and an unnamed referee for constructive comments on the manuscript, R.L. Barnett, D.M. Kingston, and T. Bonli for assistance with EMP analyses, and the Natural Sciences and Engineering Research Council of Canada for financial support.

## References cited

Brown, I.D. (1981) The bond-valence method: An empirical approach to chemical structure and bonding. In M. O'Keeffe and A. Navrotsky, Eds., Structure and bonding in crystals, vol. 2, p. 1–30. Academic, New York.

Burt, D.M. (1989) Compositional and phase relations among rare earth element minerals. In Mineralogical Society of America Reviews in Mineralogy, 21, 259–307.

Cockbain, A.G., and Smith, G.V. (1967) Alkaline-earth-rare-earth silicate and germanate apatites. Mineralogical Magazine, 36, 411–421.

Coppens, P., and Hamilton, W.C. (1970) Anisotropic extinction correction in the Zachariasen approximation. Acta Crystallographica, A26, 71–83.

Elliott, J.C., Mackie, P.E., and Young, R.A. (1973) Monoclinic hydroxyapatite. Science, 180, 1055–1057.

Fleet, M.E., and Pan, Y. (1994) Site preference of Nd in fluorapatite [$Ca_{10}(PO_4)_6F_2$]. Journal of Solid State Chemistry, 111, 78–81.

Gunawardane, R.P., Howie, R.A., and Glasser, F.P. (1982) Structure of the oxyapatite $NaY_9(SiO_4)_6O_2$. Acta Crystallographica, B38, 1564–1566.

Hamilton, W.C. (1965) Significance tests on the crystallographic *R* factor. Acta Crystallographica, 18, 502–510.

Hughes, J.M., Cameron, M., and Crowley, K.D. (1989) Structural variations in natural F, OH, and Cl apatites. American Mineralogist, 74, 870–876.

——— (1990) Crystal structures of natural ternary apatites: Solid solution in the $Ca_5(PO_4)_3X$ (X = F, OH, Cl) system. American Mineralogist, 75, 295–304.

Hughes, J.M., Cameron, M., and Mariano, A.N. (1991) Rare-earth-element ordering and structural variations in natural rare-earth-bearing apatites. American Mineralogist, 76, 1165–1173.

Hughson, M.R., and Sen Gupta, J.G. (1964) A thorian intermediate member of the britholite-apatite series. American Mineralogist, 49, 937–951.

Ibers, J.A., and Hamilton, W.C., Eds. (1974) International tables for X-ray crystallography, vol. IV, 366 p. Kynoch, Birmingham, U.K.

Kay, M.I., Young, R.A., and Posner, A.S. (1964) Crystal structure of hydroxyapatite. Nature, 204, 1050–1052.

Mackie, P.E., and Young, R.A. (1973) Location of Nd dopant in fluorapatite, $Ca_5(PO_4)_3F$:Nd. Journal of Applied Crystallography, 6, 26–31.

Mackie, P.E., Elliott, J.C., and Young, R.A. (1972) Monoclinic structure of synthetic $Ca_5(PO_4)_3Cl$, chlorapatite. Acta Crystallographica, B28, 1840–1848.

McKay, G.A. (1989) Partitioning of rare earth elements between major silicate minerals and basaltic melts. In Mineralogical Society of America Reviews in Mineralogy, 21, 45–77.

Miyawaki, R., and Nakai, I. (1993) Crystal-chemical aspects of rare-earth minerals (abs.). Mineralogical Society, London, p. 86–88.

Morss, L.R. (1976) Thermochemical properties of yttrium, lanthanum, and the lanthanide elements and ions. Chemical Reviews, 76, 827–841.

Pan, Y., and Fleet, M.E. (1990) Halogen-bearing allanite from the White River gold occurrence, Hemlo area, Ontario. Canadian Mineralogist, 28, 67–75.

Rønsbo, J.G. (1989) Coupled substitutions involving REEs and Na and Si in apatites in alkaline rocks from the Ilímaussaq intrusion, South Greenland, and the petrological implications. American Mineralogist, 74, 896–901.

Shannon, R.D. (1976) Revised effective ionic radii and systematic studies of interatomic distances in halides and chalcogenides. Acta Crystallographica, A32, 751–767.

Suitch, P.R., LaCout, J.L., Hewat, A., and Young, R.A. (1985) The structural location and role of $Mn^{2+}$ partially substituted for $Ca^{2+}$ in fluorapatite. Acta Crystallographica, B41, 173–179.

Urusov, V.S., and Khudolozhkin, V.O. (1974) An energy analysis of cation ordering in apatite. Geochemistry International, 11, 1048–1053.

Wyckoff, R.W.G. (1965) Crystal structures (2nd edition), vol. 3, 228 p. Wiley, New York.

Manuscript received July 22, 1994
Manuscript accepted November 18, 1994